Mixed Convection in a Doubly Stratified Micropolar Fluid Saturated Non-Darcy Porous Medium

D. Srinivasacharya* and Ch. RamReddy

Department of Mathematics, National Institute of Technology, Warangal 506004, Andhra Pradesh, India

The effects of thermal and solutal stratification on mixed convection along a vertical plate embedded in a micropolar fluid saturated non-Darcy porous medium are analysed. The nonlinear governing equations and their associated boundary conditions are initially cast into dimensionless forms by pseudo-similarity variables. The resulting system of equations is then solved numerically using the Keller-box method. The numerical results are compared and found to be in good agreement with previously published results as special cases of the present investigation. The velocity, microrotation, temperature and concentration profiles are shown for different values of the coupling number, non-Darcy parameter, mixed convection parameter, thermal and solutal stratification parameters. The numerical values of the skin friction, wall couple stress, heat and mass transfer rates for different values of governing parameters are also tabulated.

Keywords: mixed convection, non-Darcy porous medium, micropolar fluid, thermal stratification, solutal stratification

INTRODUCTION

The study of convective flow, heat and mass transfer in porous media has been an active field of research as it plays a crucial role in diverse applications, such as thermal insulation, extraction of crude oil and chemical catalytic reactors, etc. Considerable work has been reported on flow, heat and mass transfer in Darcian porous media. However, Darcys law is valid only for slow flows through porous media with low permeability. At higher flow rates, there is a departure from the linear law and inertial effects become important. The simultaneous effects of fluid inertia force and boundary viscous resistance on the flow and heat transfer in a porous medium were analysed by Vafai and Tien (1976) for forced convection and by Ranganathan and Viskanta (1984) for mixed convection. From their reports, it was found that both boundary and inertia effects exhibit a significant influence on velocity distribution and heat transfer and thus these effects cannot be ignored. The Darcy-Forchheimer model describes the effect of inertia as well as viscous forces in porous media. A detailed review of convective heat transfer in Darcian and non-Darcian porous medium can be found in the book by Nield and Bejan (2006). Recently, Shateyi et al. (2010) described the two-dimensional flow of an incompressible viscous fluid through a non-porous channel with heat generation and a chemical reaction.

In many problems of practical interest, natural/mixed convection flows arise in a thermally stratified environment. The input of thermal energy in enclosed fluid regions, due to the discharge of hot fluid or heat removal from heated bodies, often leads to the generation of a stable thermal stratification. Stratification of fluid arises due to temperature variations, concentration differences or the presence of different fluids. Several investigations have explored the importance of convective heat and mass transfer in doubly stratified porous media using Darcian and non-Darcian models.

Previous studies (for a comprehensive review see Gebhart et al. (1988)) have shown that stratification increases the local heat transfer coefficient and decreases the velocity and buoyancy levels. Another considerable effect of the stratification on the mean field is the formation of a region with a temperature deficit (i.e. a negative dimensionless temperature) and flow reversal in the outer part of the boundary layer. This phenomenon was first shown theoretically by Prandtl (1952) for an infinite wall and later on by Jaluria and Himasekhar (1983) for semi-infinite walls. Recently, Murthy et al. (2004), Rathish Kumar and Shalini (2005),

*Author to whom correspondence may be addressed.
E-mail addresses: dsrinivasacharya@gmail.com,dsc@nitw.ac.in
Can. J. Chem. Eng. 90:1311–1322, 2012

DOI 10.1002/cjce.20658
Published online 25 October 2011 in Wiley Online Library (wileyonlinelibrary.com).

and Lakshmi Narayana and Murthy (2006, 2007) reported that the temperature and concentration became negative in the boundary layer depending on the relative intensity of the thermal and solutal stratification.

Only few experimental studies were carried out on vertical free convection in a stratified environment. Jaluria and Gebhart (1974) studied the stability of the flow adjacent to a vertical plate dissipating a uniform heat flux into a stratified medium both theoretically and experimentally. For this case a theoretical similarity solution exists, in which the ambient stratification varies like $x^{1/5}$, where x is the downstream coordinate. Unlike the case of linear stratification, the flow reversal and temperature deficit in this case (Gebhat et al., 1988), where the variation of the ambient temperature is relatively weak, are extremely small.

The effects of heat and mass transfer in non-Newtonian fluid have great significance in engineering applications such as thermal design of industrial equipment dealing with molten plastics, polymeric liquids, foodstuffs or slurries. The combined convection flow of an Ostwald-de Waele type power–law non-Newtonian fluid past a vertical slotted surface in the presence of uniform surface heat flux, has been investigated numerically by Gorla et al. (2009). The micropolar fluid model introduced by Eringen (1966) exhibits some microscopic effects arising from the local structure and micromotion of the fluid elements. Further, they can sustain couple stresses. Micropolar fluids have been shown to accurately simulate the flow characteristics of polymeric additives, geomorphological sediments, colloidal suspensions, haematological suspensions, liquid crystals, lubricants, etc. The main advantage of using micropolar fluid model compared to other non-Newtonian fluids is that it takes care of the rotation of fluid particles by means of an independent kinematic vector called the microrotation vector.

The problem of mixed convection heat and mass transfer along a vertical surface submerged in a micropolar fluid has been studied by a number of investigators. Mixed convection boundary layer flow of a micropolar fluid from an isothermal vertical flat plate has been analysed by Jena and Mathur (1984). Asymptotic boundary layer solutions are presented for the combined convection from a vertical semi-infinite plate to a micropolar fluid by Gorla et al. (1990). Wang (1998) examined the effect of wall conduction on laminar mixed convection heat transfer of micropolar fluids along a vertical flat plate. Chang and Lee (2008) analysed flow and heat transfer characteristics of the free convection on a vertical plate with uniform and constant heat flux in a thermally stratified micropolar fluid. An analysis has been carried out to obtain the effects of higher order chemical reaction on flow and mass transfer characteristics of micropolar fluids past a nonlinear permeable stretching sheet immersed in a porous medium with variable concentration of the reactant by Rahman and Al-Lawatia (2010). Srinivasacharya and RamReddy (2010) studied the natural convection heat and mass transfer along a vertical plate embedded in a doubly stratified micropolar fluid saturated non-Darcy porous medium. Recently, Motsa et al. (2010) solved the problem of steady viscous flow of a micropolar fluid driven by injection between two porous disks using novel spectral modification of the homotopy analysis method (SHAM).

When heat and mass transfer occur simultaneously in a moving fluid, the relations between the fluxes and the driving potentials are of a more intricate nature. It has been observed that an energy flux can be generated not only by temperature gradients but also by concentration gradients. The energy flux caused by a concentration gradient is termed the diffusion-thermo (Dufour) effect. On the other hand, mass fluxes can also be created by temperature gradients and this embodies the thermal-diffusion (Soret) effect. Dufour and Soret effects on heat and mass transfer in a non-Newtonian micropolar fluid in a horizontal channel have been presented by Awad and Sibanda (2010). Recently, Srinivasacharya and RamReddy (2011) have studied the Soret and Dufour effects on the steady, laminar mixed convection heat and mass transfer along a semi-infinite vertical plate embedded in a non-Darcy porous medium saturated with micropolar fluid. The Soret and Dufour effects are usually minor and can be neglected in simple models of coupled heat and mass transfer.

The effects of thermal and mass stratification on the mixed convection heat and mass transfer along a vertical plate in a fluid saturated non-Darcy porous medium are discussed by Murthy et al. (2007). They assumed that the medium is linearly stratified with respect to both temperature and concentration and neglected the viscous resistance due to the solid boundary. The mixed convection on a vertical plate in a micropolar fluid in the presence of thermal and solutal stratification with non-Darcy effects has not been reported in the literature. The aim of this investigation is to consider the effects of thermal and mass stratification on the mixed convection heat and mass transfer along a vertical plate in a micropolar fluid saturated non-Darcy porous medium. We assumed that the wall temperature and concentration are constants and the medium is linearly stratified with respect to both temperature and concentration. This type of investigation is useful in understanding heat and mass transfer characteristics around a hot radioactive subsurface storage site or around a cooling magmatic intrusion where the theory of convection heat and mass transport is involved. Hence, these boundary conditions are physically realistic and have more practical relevance. The Keller-box method given in Cebeci and Bradshaw (1984) is employed to solve the nonlinear system of this particular problem. The effects of micropolar, non-Darcy, mixed convection, thermal and mass stratification parameters are examined and are displayed through graphs. The results are compared with relevant results in the existing literature and are found to be in good agreement.

MATHEMATICAL FORMULATION

Consider the steady mixed convection heat and mass transfer along a vertical plate embedded in a stable, a doubly stratified micropolar fluid saturated non-Darcy porous medium. The porous medium is considered to be homogeneous and isotropic (i.e. uniform with a constant porosity and permeability) and is saturated with a fluid which is in local thermodynamic equilibrium with the solid matrix. The fluid has constant properties except the density in the buoyancy term of the balance of momentum equation. The fluid flow is moderate, so the pressure drop is proportional to the linear combination of fluid velocity and the square of velocity (Forchhiemer flow model is considered).

The free stream velocity which is parallel to the vertical plate is u_∞, temperature is $T_{\infty,0}$ and concentration is $C_{\infty,0}$. Choose the coordinate system such that x-axis is along the vertical plate and y-axis normal to the plate. The physical model and coordinate system are shown in Figure 1. The plate is maintained at uniform wall temperature T_w and concentration C_w. The ambient medium is assumed to be vertically linearly stratified with respect to both temperature and concentration in the form $T_\infty(x) = T_{\infty,0} + Ax$ and $C_\infty(x) = C_{\infty,0} + Bx$ respectively, where A and B are constants and varied to alter the intensity of stratification in the medium. The values of T_w and C_w are assumed to be greater than the

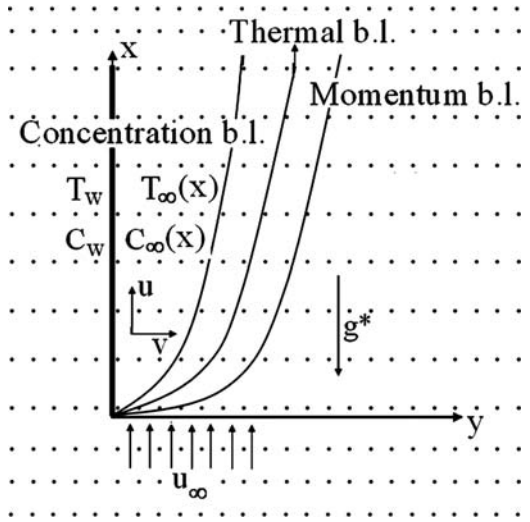

Figure 1. Physical model and coordinate system.

ambient temperature $T_{\infty,0}$ and concentration $C_{\infty,0}$ at any arbitrary reference point in the medium (inside the boundary layer).

By employing laminar boundary layer flow assumptions, Boussinesq approximation, using the Darcy-Forchheimer model and Dupuit-Forchheimer relationship (Nield and Bejan, 2006), the governing equations for the micropolar fluid are given by:

$$\frac{\partial u}{\partial x}+\frac{\partial v}{\partial y}=0 \tag{1}$$

$$\frac{\rho}{\varepsilon^2}\left(u\frac{\partial u}{\partial x}+v\frac{\partial u}{\partial y}\right)+\frac{\mu}{K_P}(u-u_\infty)+\frac{\rho b}{K_P}\left(u^2-u_\infty^2\right)=\left(\frac{\mu+\kappa}{\varepsilon}\right)\frac{\partial^2 u}{\partial y^2}+\kappa\frac{\partial \omega}{\partial y}+\rho g^*(\beta_T(T-T_\infty)+\beta_C(C-C_\infty)) \tag{2}$$

$$\frac{\rho j}{\varepsilon}\left(u\frac{\partial \omega}{\partial x}+v\frac{\partial \omega}{\partial y}\right)=\gamma\frac{\partial^2\omega}{\partial y^2}-\kappa\left(2\omega+\frac{1}{\varepsilon}\frac{\partial u}{\partial y}\right) \tag{3}$$

$$u\frac{\partial T}{\partial x}+v\frac{\partial T}{\partial y}=\alpha\frac{\partial^2 T}{\partial y^2} \tag{4}$$

$$u\frac{\partial C}{\partial x}+v\frac{\partial C}{\partial y}=D\frac{\partial^2 C}{\partial y^2} \tag{5}$$

where u and v are the Darcy velocity components in x and y directions respectively, ω is the component of microrotation whose direction of rotation lies in the xy-plane, T is the temperature, C is the concentration, g^* is the acceleration due to gravity, K_p is the permeability, b is the empirical constant associated with the Forchheimer porous inertia term, ε is the porosity, ρ is the density, μ is the dynamic coefficient of viscosity, β_T is the coefficient of thermal expansion, β_C is the coefficient of solutal expansions, κ is the vortex viscosity, j is the microinertia density, γ is the spin-gradient viscosity, α and D are the effective thermal and solutal diffusivities of the porous medium. The second and third terms on the left hand side of Equation (2) stand for the first-order (Darcy) resistance and second-order porous inertia resistance respectively.

The boundary conditions are:

$$u=0,\ v=0,\ \omega=0,\ T=T_w,\ C=C_w \quad \text{at} \quad y=0 \tag{6a}$$

$$u=u_\infty,\ \omega=0,\ T=T_\infty(x),\ C=C_\infty(x) \quad \text{as} \quad y\to\infty \tag{6b}$$

where the subscripts w, $(\infty,0)$ and ∞ indicate the conditions at the wall, at some reference point in the medium, and at the outer edge of the boundary layer respectively. The boundary condition $\omega=0$ in (6a) represents the case of concentrated particle flows in which the microelements close to the wall are not able to rotate.

In view of the continuity Equation (1), we introduce the stream function ψ by:

$$u=\frac{\partial\psi}{\partial y},\quad v=-\frac{\partial\psi}{\partial x} \tag{7}$$

Substituting Equation (7) in Equations (2)–(5) and then using the following pseudo-similarity transformations:

$$\left.\begin{gathered}\xi=\tfrac{x}{L},\ \eta=\left(\tfrac{\mathrm{Re}}{\xi}\right)^{1/2}\tfrac{y}{L},\ f(\xi,\eta)=\left(\tfrac{\mathrm{Re}}{\xi}\right)^{1/2}\tfrac{\psi}{Lu_\infty},\ g(\xi,\eta)=\left(\tfrac{\xi}{\mathrm{Re}}\right)^{1/2}\tfrac{L\omega}{u_\infty}\\ \theta(\xi,\eta)=\tfrac{T-T_{\infty,0}}{T_w-T_{\infty,0}}-\tfrac{Ax}{T_w-T_{\infty,0}},\ \phi(\xi,\eta)=\tfrac{C-C_{\infty,0}}{C_w-C_{\infty,0}}-\tfrac{Bx}{C_w-C_{\infty,0}}\end{gathered}\right\} \tag{8}$$

we get the following nonlinear system of differential equations:

$$\left(\frac{1}{\varepsilon(1-N)}\right)f'''+\frac{1}{2\varepsilon^2}f\,f''+\left(\frac{N}{1-N}\right)g'+\xi\,Ri(\theta+\mathcal{B}\,\phi)+\frac{1}{Da\,\mathrm{Re}}\xi(1-f')+\frac{Fs}{Da}\xi(1-f'^2)=\frac{\xi}{\varepsilon^2}\left(f'\frac{\partial f'}{\partial\xi}-f''\frac{\partial f}{\partial\xi}\right) \tag{9}$$

$$\lambda g''+\frac{1}{2\varepsilon}(f\,g'+f'\,g)-\left(\frac{N}{1-N}\right)J\,\xi\left(2g+\frac{1}{\varepsilon}f''\right)=\frac{\xi}{\varepsilon}\left(f'\frac{\partial g}{\partial\xi}-g'\frac{\partial f}{\partial\xi}\right) \tag{10}$$

$$\frac{1}{\mathrm{Pr}}\theta''+\frac{1}{2}f\theta'-\varepsilon_1\xi f'=\xi\left(f'\frac{\partial\theta}{\partial\xi}-\theta'\frac{\partial f}{\partial\xi}\right) \tag{11}$$

$$\frac{1}{Sc}\phi''+\frac{1}{2}f\phi'-\varepsilon_2\xi f'=\xi\left(f'\frac{\partial\phi}{\partial\xi}-\phi'\frac{\partial f}{\partial\xi}\right) \tag{12}$$

where the primes indicate partial differentiation with respect to η alone, $\mathrm{Re}=((u_\infty L)/\nu)$ is the Reynolds number, $Gr=\left(\left(g^*\beta_T(T_w-T_{\infty,0})L^3\right)/\nu^2\right)$ is the thermal Grashof number, $\mathrm{Da}=(K_P/L^2)$ is the Darcy number, $Fs=(b/L)$ is the Forchheimer number, $\mathrm{Pr}=(\nu/\alpha)$ is the Prandtl number, $Sc=(\nu/D)$ is the Schmidt number, $J=\dfrac{L^2}{j\,\mathrm{Re}}$ is the microinertia density, $\lambda=(\gamma/(j\rho\nu))$ is the spin-gradient viscosity and $N=(\kappa/(\kappa+\mu))$ $(0\le N<1)$ is the Coupling number (Cowin, 1968). $Ri=((Gr)/(Re^2))$ is the mixed convection parameter, $\mathcal{B}=\dfrac{\beta_C\left(C_w-C_{\infty,0}\right)}{\beta_T\left(T_w-T_{\infty,0}\right)}$ is the buoyancy ratio. $\varepsilon_1=((AL)/(T_w-T_{\infty,0}))$ and $\varepsilon_2=((BL)/C_w-C_{\infty,0})$ are the thermal and solutal stratification parameters.

The boundary conditions (6) in terms of f, g, θ and ϕ become:

$$\eta = 0 : f'(\xi, 0) = 0,\ f(\xi, 0) = -2\xi\left(\frac{\partial f}{\partial \xi}\right)_{\eta=0},$$
$$g(\xi, 0) = 0,\ \theta(\xi, 0) = 1-\varepsilon_1\xi,\ \phi(\xi, 0) = 1-\varepsilon_2\xi \tag{13a}$$

$$\eta \to \infty : f'(\xi, \infty) = 1,\ g(\xi, \infty) = 0,\ \theta(\xi, \infty) = 0,\ \phi(\xi, \infty) = 0 \tag{13b}$$

The wall shear stress and the wall couple stress are:

$$\tau_w = \left[(\mu + \kappa)\frac{\partial u}{\partial y} + \kappa\omega\right]_{y=0}, \quad m_w = \gamma\left[\frac{\partial \omega}{\partial y}\right]_{y=0} \tag{14}$$

and the heat and mass transfers from the plate respectively are given by:

$$q_w = -k\left(\frac{\partial T}{\partial y}\right)_{y=0}, \quad q_m = -D\left(\frac{\partial C}{\partial y}\right)_{y=0} \tag{15}$$

The dimensionless skin friction $C_f = \left((2\tau_w)/\left(\rho U_*^2\right)\right)$, wall couple stress $M_w = \left((m_w)/\left(\rho U_*^2 L\right)\right)$, the local Nusselt number $Nu_x = ((q_w x)/(k(T_w - T_{\infty,0})))$ and local Sherwood number $Sh_x = ((q_m x)/(D(C_w - C_{\infty,0})))$, where U_* is the characteristic velocity, are given by:

$$C_f\ \mathrm{Re}_x^{1/2} = \left(\frac{2}{1-N}\right) f''(\xi, 0), \qquad M_w\ \mathrm{Re}_x = \left(\frac{\lambda}{J}\right) g'(\xi, 0) \tag{16a}$$

$$\frac{Nu_x}{\mathrm{Re}_x^{1/2}} = -\theta'(\xi, 0), \quad \frac{Sh_x}{\mathrm{Re}_x^{1/2}} = -\phi'(\xi, 0) \tag{16b}$$

where $\mathrm{Re}_x = ((u_\infty x)/\nu)$ is the local Reynolds number.

RESULTS AND DISCUSSIONS

The flow Equations (9) and (10) which are coupled, together with the energy and concentration Equations (11) and (12), constitute nonlinear non-homogeneous differential equations for which closed form solutions cannot be obtained and hence we have to solve the problem numerically. Hence the governing boundary layer Equations (9)–(12) have been solved numerically using the Keller-box implicit method discussed in book by Cebeci and Bradshaw (1984). This method has been proven to be adequate and give accurate results for boundary layer equations. In the present study, the boundary conditions for η at ∞ are replaced by a sufficiently large value of η where the velocity approaches one and the microrotation, temperature and concentration profiles approach zero. We have taken $\eta_\infty = 8$ and a grid size of η of 0.01. We have computed the solutions for the dimensionless velocity, angular momentum, temperature and concentration function as shown graphically in Figures 2a–6d. The effects of micropolar parameter N, non-Darcy parameter Fs, Ri and stratification parameters, ε_1 and ε_2 have been discussed.

In the present study, we have adopted the following default parameter values for the numerical computations: $B = 1.0$, $Re = 200$, $Da = 0.1$, $\varepsilon = 0.6$, $Pr = 0.71$, $Sc = 0.22$ and $\xi = 0.1$. The values of micropolar parameters $J = 0.01$ and $\lambda = 0.5$ are chosen so as to satisfy the thermodynamic restrictions on the material parameters given by Eringen (1966). These values are used throughout the computations, unless otherwise indicated.

The case of the mixed convection flow of Newtonian fluids along a vertical flat plate of Lloyd and Sparrow (1970) can be obtained by taking $N = 0$, $\varepsilon_1 = 0$, $\varepsilon_2 = 0$, $\varepsilon = 1$, $Da \to \infty$ and $B = 0$.

Thus, in the absence of coupling number N, buoyancy ratio B, stratification parameters ε_1 and ε_2 with $\varepsilon = 1$, $Da \to \infty$, $J = 0$, $\lambda = 0$, $\xi = 1$ and using the principle of local similarity, the results of the governing Equations (1)–(5) have been compared with the special case of (Lloyd and Sparrow, 1970) and it is found that they are in good agreement, as shown in Table 1. Therefore, the developed code can be used with great confidence to study the problem considered in this study.

The coupling number N characterises the coupling of linear and rotational motion arising from the micromotion of the fluid molecules. Hence N signifies the coupling between the Newtonian and rotational viscosities. As N tends to one the effect of microstructure becomes significant, whereas with a small value of N the individuality of the substructure is much less pronounced. As κ tend to zero, N also tends to zero, the micropolarity is lost and the fluid is to behave as non-polar fluid.

In Figure 2a–d, the effects of the coupling number N on the dimensionless velocity, microrotation, temperature and concentration profiles are presented for fixed values of Fs, Ri, ε_1 and ε_2. The case of $N = 0$ corresponds to Newtonian fluid flow where microrotational effects vanish. The velocity in case of micropolar fluid is less compared to the case of viscous fluid. It can be observed from Figure 2a that the maximum velocity decreases in amplitude as N increases and the location of the maximum velocity moves farther away from the wall. From Figure 2b, it can be seen that the microrotation changes in sign from negative to positive within the boundary layer. Also, it is clear that the magnitude of the microrotation increases with an increase in coupling number N. From Figure 2c, we see that the temperature boundary layer thickness increases with the increase of coupling number N. It can be seen from Figure 2d that the concentration boundary layer thickness of the fluid increases with the increase of coupling number N. Furthermore, the temperature and concentration in case of micropolar fluids is more than that of the corresponding Newtonian fluid case.

The dimensionless velocity distribution for different values of Fs with $N = 0.3$, $Ri = 2.0$, $\varepsilon_1 = 0.05$ and $\varepsilon_2 = 0.05$ is depicted in Figure 3a. Since Fs represent the inertial drag, thus an increase in the Forchheimer number increases the resistance to the flow and so a decrease in the fluid velocity ensues. Here $Fs = 0$ represents the case where the flow is Darcian. The velocity is maximum in this case due to the total absence of inertial drag. From Figure 3b, it can be observed that the microrotation changes in sign from negative to positive within the boundary layer. The dimensionless temperature for different values of Forchheimer number for $N = 0.3$, $Ri = 2.0$, $\varepsilon_1 = 0.05$ and $\varepsilon_2 = 0.05$, is displayed in Figure 3c. An increase in Fs, increase temperature values, since as the fluid is decelerated, energy is dissipated as heat and serves to increase temperatures. As such the temperature is minimised for the lowest value of Fs and maximised for the highest value of Fs as shown in Figure 3c. Figure 3d demonstrates the dimensionless concentration for different values of Forchheimer number with $N = 0.3$, $Ri = 2.0$, $\varepsilon_1 = 0.05$ and $\varepsilon_2 = 0.05$. As the Forchheimer number increases, the concentration boundary layer thickness increases. The increase in non-Darcy parameter reduces the intensity of the flow but enhance the thermal and concentration boundary layer thicknesses.

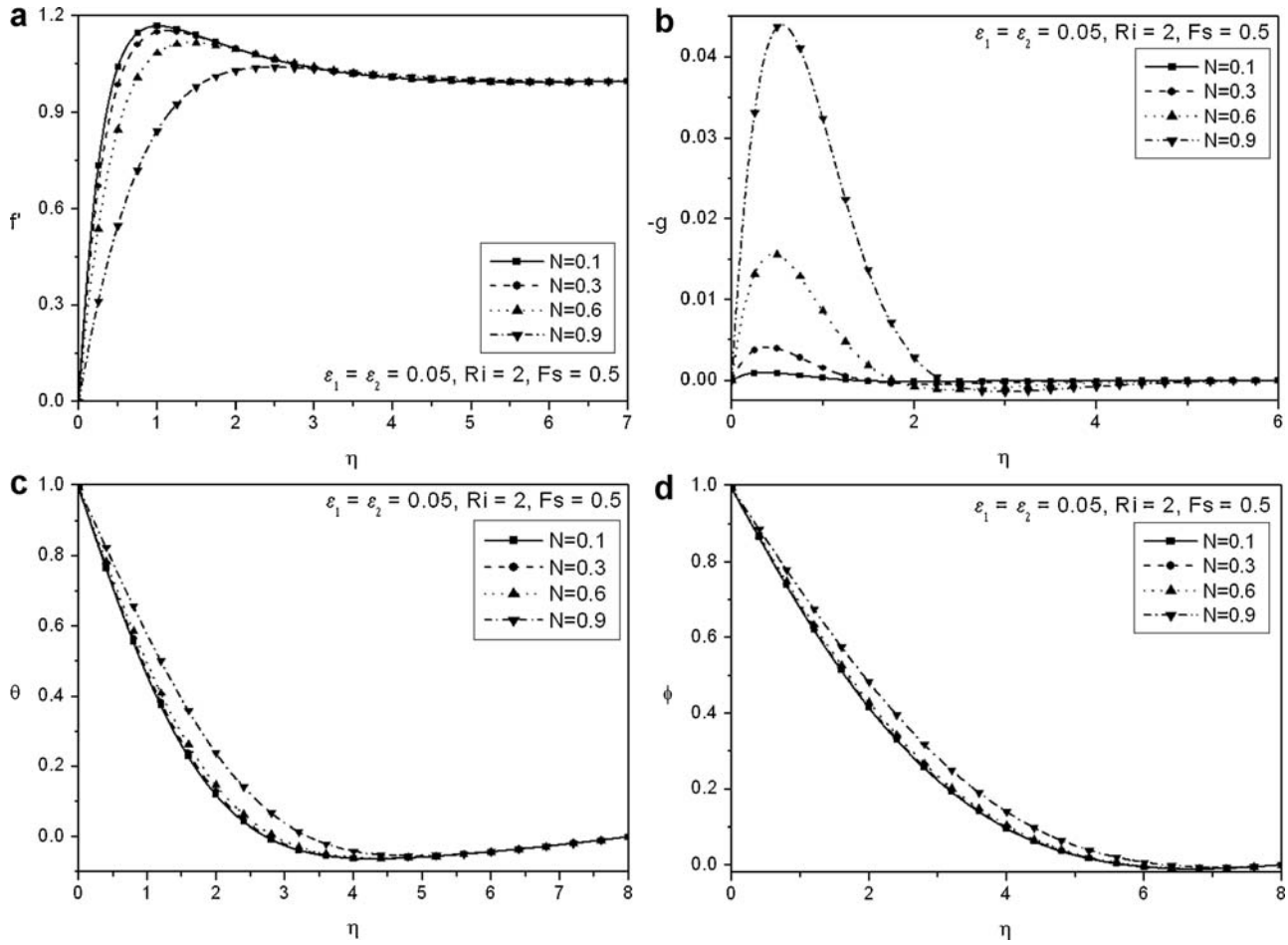

Figure 2. Effect of coupling number (*N*) on the (a) velocity, (b) microrotation, (c) temperature and (d) concentration.

Figure 4a shows the dimensionless velocity profile for various values of the *Ri* with fixed values of *N*, *Fs*, ε_1 and ε_2. It reveals that as the value of *Ri* increases, the dimensionless velocity rises. Compared with the limiting case of $Ri = 0.0$ (i.e. pure forced convection), an increase in the value of *Ri* gives rise to a higher velocity. Since a greater value of *Ri* indicates a greater buoyancy effects in mixed convection flow leads to an acceleration of the fluid flow. From Figure 4b, we see that the microrotation changes in sign from negative to positive within the boundary layer. Figure 4c illustrates the dimensionless temperature for selected values of *Ri*. The results indicate that the dimensionless temperature reduces with the increase of *Ri*. The temperature in case of mixed convection is less compared to that of pure forced convection. As *Ri* (i.e. buoyancy effects) increase, the convection cooling effect increases and hence the temperature reduces. The effect of *Ri* on the dimensionless concentration is depicted in Figure 4d. It is clear that the concentration of the fluid decreases with the increase of *Ri*.

Figure 5a displays the non-dimensional velocity for different values of thermal stratification parameter ε_1 for fixed values of *N*, *Fs*, *Ri* and ε_2. Also, it can be noted that the velocity of the fluid decreases with the increase of thermal stratification parameter. This is because of thermal stratification reduces the effective

Table 1. Comparison of $Nu_x Re_x^{-1/2}$ for mixed convection between a vertical flat plate and Newtonian fluids (Lloyd and Sparrow, 1970)

	Pr = 0.72		*Pr* = 10		*Pr* = 100	
Ri	Lloyd and Sparrow (1970)	Present	Lloyd and Sparrow (1970)	Present	Lloyd and Sparrow (1970)	Present
0.00	0.2956	0.2956	0.7281	0.7281	1.5720	1.5752
0.01	0.2979	0.2979	0.7313	0.7313	1.5750	1.5787
0.04	0.3044	0.3044	0.7404	0.7408	1.5850	1.5889
0.10	0.3158	0.3158	0.7574	0.7578	1.6050	1.6083
0.40	0.3561	0.3561	0.8259	0.8263	1.6910	1.6945
1.00	0.4058	0.4058	0.9212	0.9217	1.8260	1.8303
2.00	0.4584	0.4584	1.0290	1.0300	1.9940	1.9994
4.00	0.5258	0.5258	1.1730	1.1740	2.2320	2.2395

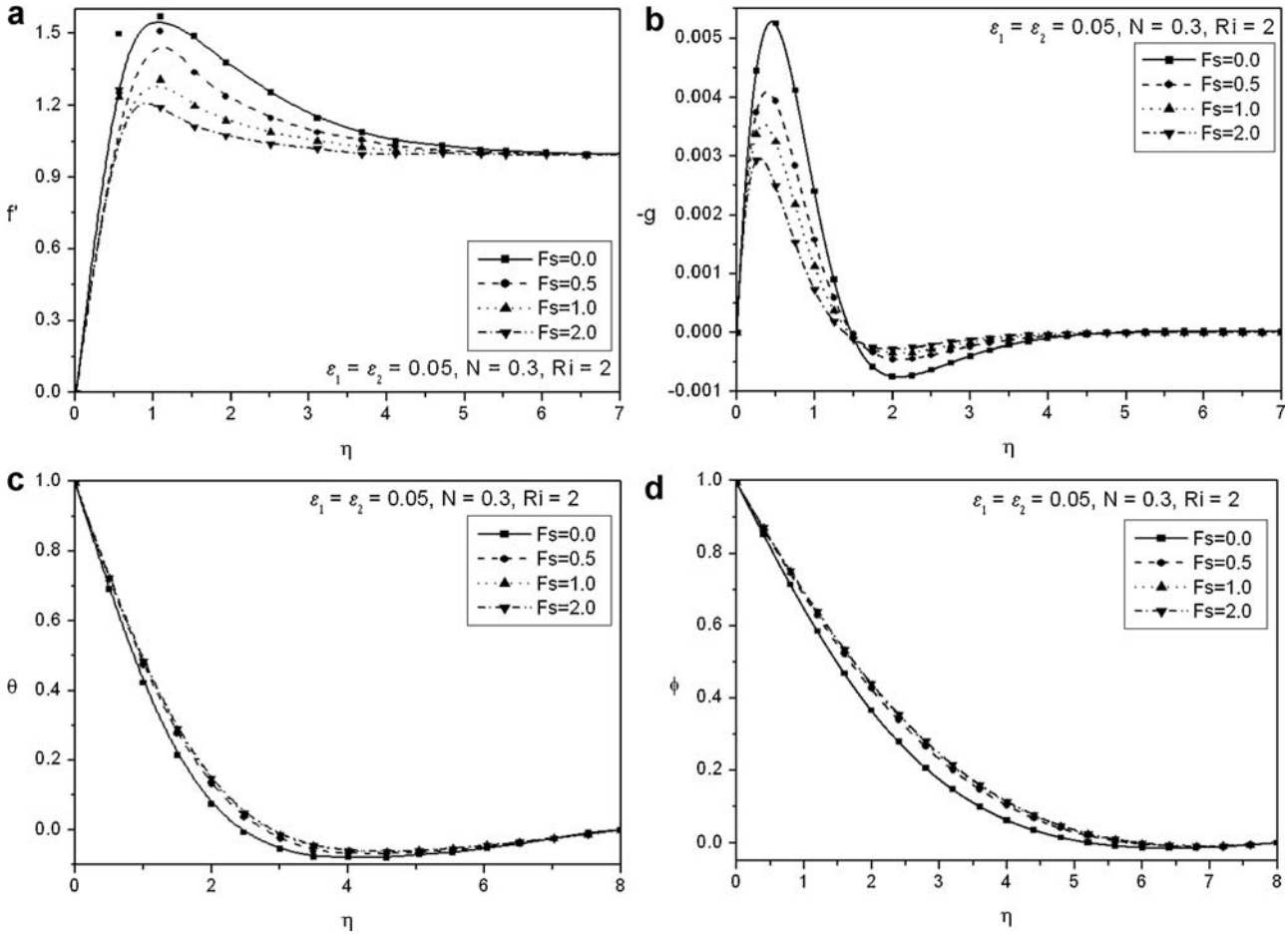

Figure 3. Effect of Forchheimer number (*Fs*) on the (a) velocity, (b) microrotation, (c) temperature and (d) concentration.

convective potential between the heated plate and the ambient fluid in the medium. Hence, the thermal stratification effect reduces the velocity in the boundary layer. From Figure 5b, we observe that the microrotation changes in sign from negative to positive within the boundary layer as thermal stratification parameter enhances. The dimensionless temperature for different values of thermal stratification parameter for $N = 0.3$, $Fs = 0.5$, $Ri = 2$ and $\varepsilon_2 = 0.05$, is shown in Figure 5c. It is evident that the temperature of the fluid decreases with the increase of thermal stratification parameter. When the thermal stratification effect is taken into consideration, the effective temperature difference between the plate and the ambient fluid will decrease; therefore, the thermal boundary layer is thickened and the temperature is reduced. Figure 5d depicts the dimensionless concentration for different values of thermal stratification parameter for $N = 0.3$, $Fs = 0.5$, $Ri = 2$ and $\varepsilon_2 = 0.05$. It is seen that the concentration of the fluid increases with the increase of thermal stratification parameter. It can be noted that the effect of the stratification on the temperature is the formation of a region with a temperature deficit (i.e. a negative dimensionless temperature). This is in tune with the observation made in these studies (Prandtl, 1952; Jaluria and Himasekhar, 1983; Gebhart et al., 1988; Murthy et al., 2004; Lakshmi Narayana and Murthy, 2006).

The dimensionless velocity component for different values of solutal stratification parameter ε_2 with fixed values of $N = 0.3$, $Fs = 0.5$, $Ri = 2$ and $\varepsilon_1 = 0.05$, is depicted in Figure 6a. It is observed that the velocity of the fluid decreases with the increase of solutal stratification parameter. From Figure 6b, we notice that the microrotation changes in sign from negative to positive within the boundary layer as solutal stratification increases. The reason is that the microrotation field in this region is dominated by a small number of particles spins that are generated by collisions with the boundary. Hence, it is showing a reverse rotation near the two boundaries. The dimensionless temperature for different values of solutal stratification parameter for $N = 0.3$, $Fs = 0.5$, $Ri = 2$ and $\varepsilon_1 = 0.05$, is displayed in Figure 6c. It is evident that the temperature of the fluid increases with the increase of solutal stratification parameter. Figure 6d demonstrates the dimensionless concentration for different values of solutal stratification parameter with $N = 0.3$, $Fs = 0.5$, $Ri = 2$ and $\varepsilon_2 = 0.05$. It is clear that the concentration of the fluid decreases with the increase of thermal stratification parameter.

Table 2 shows the effects of the coupling number N on the skin friction parameter $f''(\xi,0)$ and the dimensionless wall couple stress $g'(\xi,0)$. It shows that the skin friction factor is lower for micropolar fluid than the Newtonian fluids ($N = 0$). Since micropolar fluids offer a great resistance (resulting from vortex viscosity) to the fluid motion and causes larger skin friction factor compared to Newtonian fluid. The results also indicate that the large values of coupling number N, lower wall couple stresses. From the Table 2, we observe that the local skin friction factor $f''(\xi,0)$ enhances and the wall couple stress $g'(\xi,0)$ reduces as Fs enhances. Table 2 illustrates the effects of the Ri on the skin friction parameter $f''(\xi,0)$ and the dimensionless wall couple stress $g'(\xi,0)$. It is seen

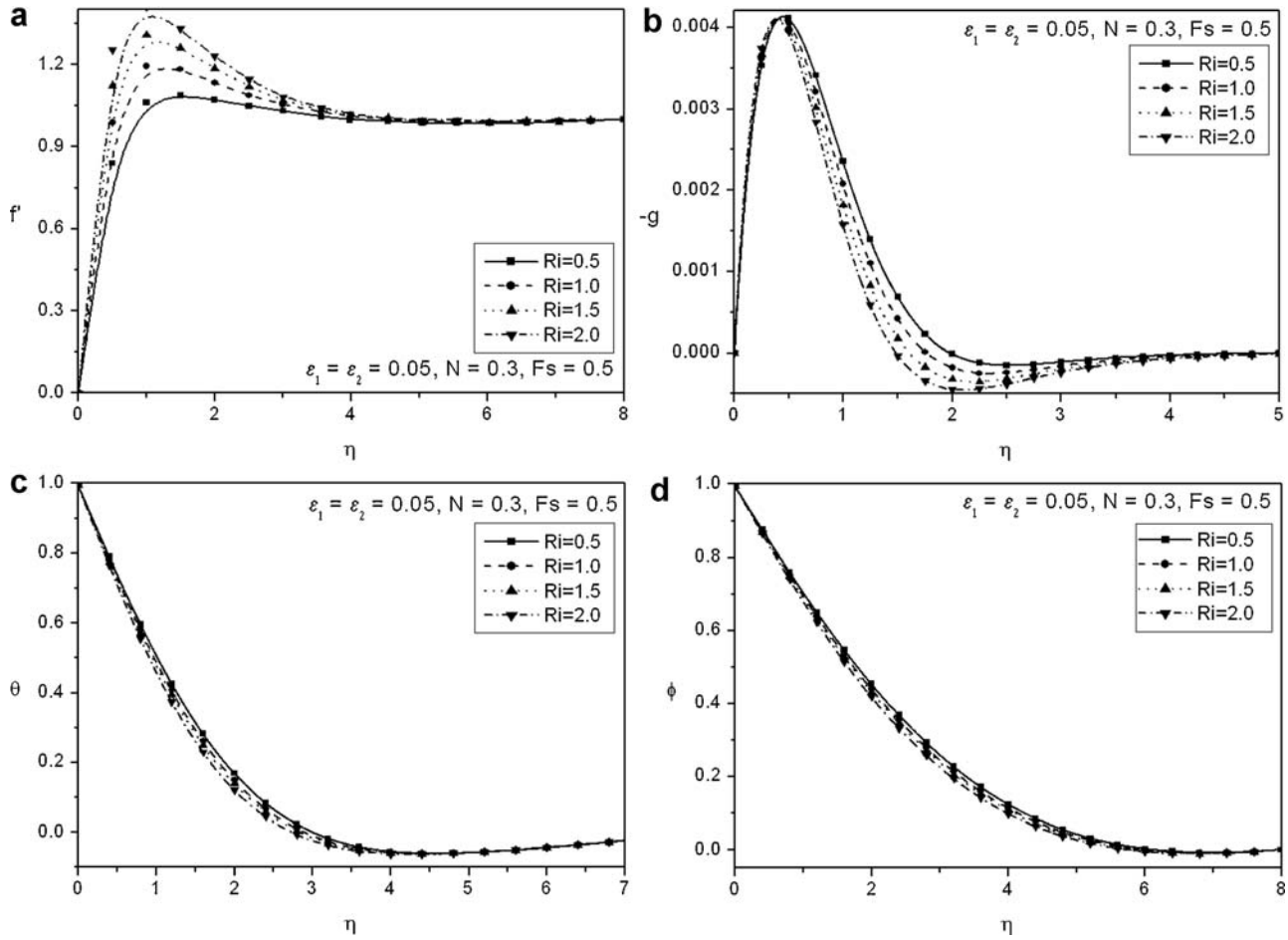

Figure 4. Effect of mixed convection parameter (*Ri*) on the (a) velocity, (b) microrotation, (c) temperature and (d) concentration.

Table 2. Effect of skin friction and wall couple stress for various values of *N*, *Fs*, *Ri*, ε_1 and ε_2

N	*Fs*	*Ri*	ε_1	ε_2	f″(ξ ,0)	− g′(ξ ,0)
0.0	0.5	1.0	0.05	0.05	3.6841	0.0000
0.1	0.5	1.0	0.05	0.05	3.4904	0.0065
0.4	0.5	1.0	0.05	0.05	3.0674	0.0241
0.6	0.5	1.0	0.05	0.05	2.2950	0.0769
0.9	0.5	1.0	0.05	0.05	1.2013	0.2808
0.3	0.0	1.0	0.05	0.05	1.7967	0.0218
0.3	0.5	1.0	0.05	0.05	3.0674	0.0241
0.3	1.0	1.0	0.05	0.05	3.9399	0.0250
0.3	1.5	1.0	0.05	0.05	4.6578	0.0256
0.3	2.0	1.0	0.05	0.05	5.2687	0.0260
0.3	0.5	0.0	0.05	0.05	2.4706	0.0217
0.3	0.5	0.5	0.05	0.05	2.7741	0.0230
0.3	0.5	1.0	0.05	0.05	3.0674	0.0241
0.3	0.5	1.5	0.05	0.05	3.3519	0.0252
0.3	0.5	2.0	0.05	0.05	3.6288	0.0263
0.3	0.5	1.0	0.00	0.05	3.0768	0.0242
0.3	0.5	1.0	0.05	0.05	3.0674	0.0241
0.3	0.5	1.0	0.10	0.05	3.0580	0.0240
0.3	0.5	1.0	0.15	0.05	3.0391	0.0238
0.3	0.5	1.0	0.40	0.05	3.0015	0.0235
0.3	0.5	1.0	0.05	0.00	3.0734	0.0242
0.3	0.5	1.0	0.05	0.10	3.0613	0.0241
0.3	0.5	1.0	0.05	0.20	3.0492	0.0240
0.3	0.5	1.0	0.05	0.30	3.0371	0.0239
0.3	0.5	1.0	0.05	0.50	3.0129	0.0237

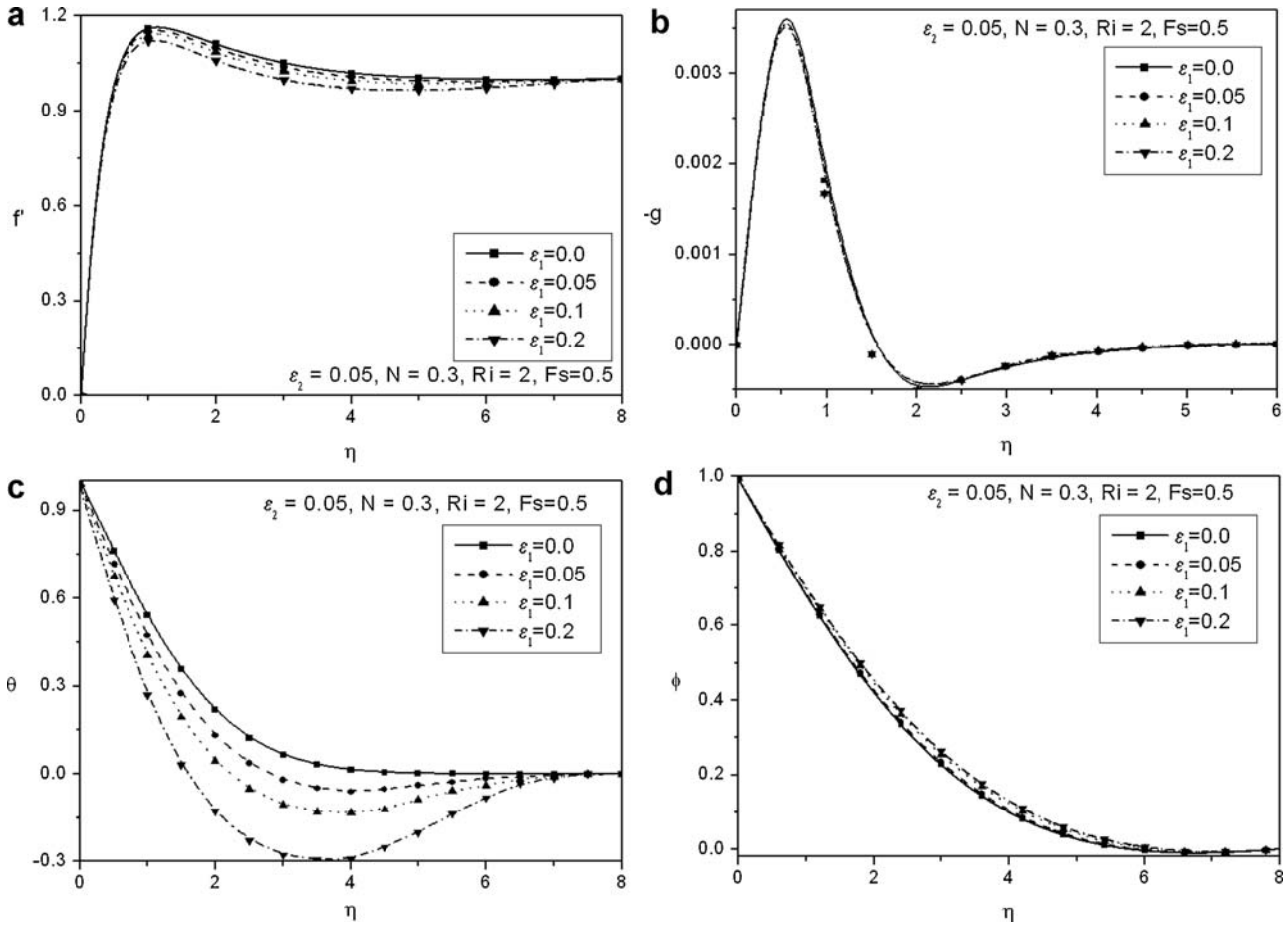

Figure 5. Effect of thermal stratification parameter (ε_1) on the (a) velocity, (b) microrotation, (c) temperature and (d) concentration.

that the local skin friction factor increases as *Ri* increases. The reason is that an increase in the buoyancy effect in mixed convection flow leads to an acceleration of the fluid flow, which increases the local skin friction factor. Also, it is found that the wall couple stress decrease with increase of the *Ri*. This observation is consistent with the velocity, microrotation, temperature and concentration distributions presented in Figure 4a–d. The effects of the thermal stratification parameter ε_1, on the skin friction parameter $f''(\xi,0)$ and the dimensionless wall couple stress $g'(\xi,0)$, are presented in Table 2. It demonstrates that the skin friction parameter decreases while the wall couple stress increases as ε_1 increases. The results of Table 2 describe the effect of solutal stratification parameter ε_2, on the skin friction parameter $f''(\xi,0)$ and the dimensionless wall couple stress $g'(\xi,0)$. It is clear that the skin friction parameter decreases but the wall couple stress increases as ε_2 increases. Furthermore, the skin friction parameter is higher and wall couple stress parameter is lower for the unstratified fluid (i.e. $\varepsilon_1 = \varepsilon_2 = 0$) than for the stratified fluid (i.e. $\varepsilon_1 > 0$ and $\varepsilon_2 \neq 0$).

Table 3 displays the effect of coupling number *N* on the non-dimensional heat and mass transfer coefficients with variation of the thermal stratification parameter ε_1 and solutal stratification parameter ε_2 for fixed $Fs = 0.5$ and $Ri = 1$. It can be seen that the heat transfer coefficient increases with the increase of ε_1 for fixed values of *N*. Physically, positive values of the stratification parameter have the tendency to decrease the boundary layer thickness due to the reduction in the temperature difference between the plate and the free stream. This causes increases in the Nusselt number as shown in Table 3. The decrease in the mass transfer coefficient causes with the increase of ε_1 for fixed values of *N* and ε_2 due to the effective mass transfer between the plate and the ambient medium decreases as the thermally stratified effect increases. The reverse trend can be observed in the case of ε_2. Also, for fixed values of both ε_1 and ε_2, the heat and mass transfer coefficients decrease with the increase of coupling number *N*. Further, it can be noticed that the heat and mass transfer coefficients are more in case of viscous fluids. This is because that as *N* increases, the thermal and solutal boundary layer thickness become large, thus give rise to a small values of local heat and mass transfer rates. Since the skin friction coefficient as well as heat and mass transfer rates are lower in the micropolar fluid comparing to the Newtonian fluid, which may be beneficial in flow, temperature and concentration control of polymer processing. Therefore, the presence of microscopic effects arising from the local structure and micromotion of the fluid elements reduce the heat and mass transfer coefficients.

The effect of non-Darcy parameter *Fs* on the non-dimensional heat and mass transfer coefficients with variation of the thermal stratification parameter ε_1 and solutal stratification parameter ε_2 for fixed $N = 0.3$ and $Ri = 2$ is presented in Table 4. It can be observed that the heat transfer coefficient increases, whereas the mass transfer coefficient decreases with the increase of ε_1 for fixed values of *Fs* and ε_2. The reverse trend can be found in the case of ε_2. The effects of buoyancy parameter *Ri* on the non-dimensional heat

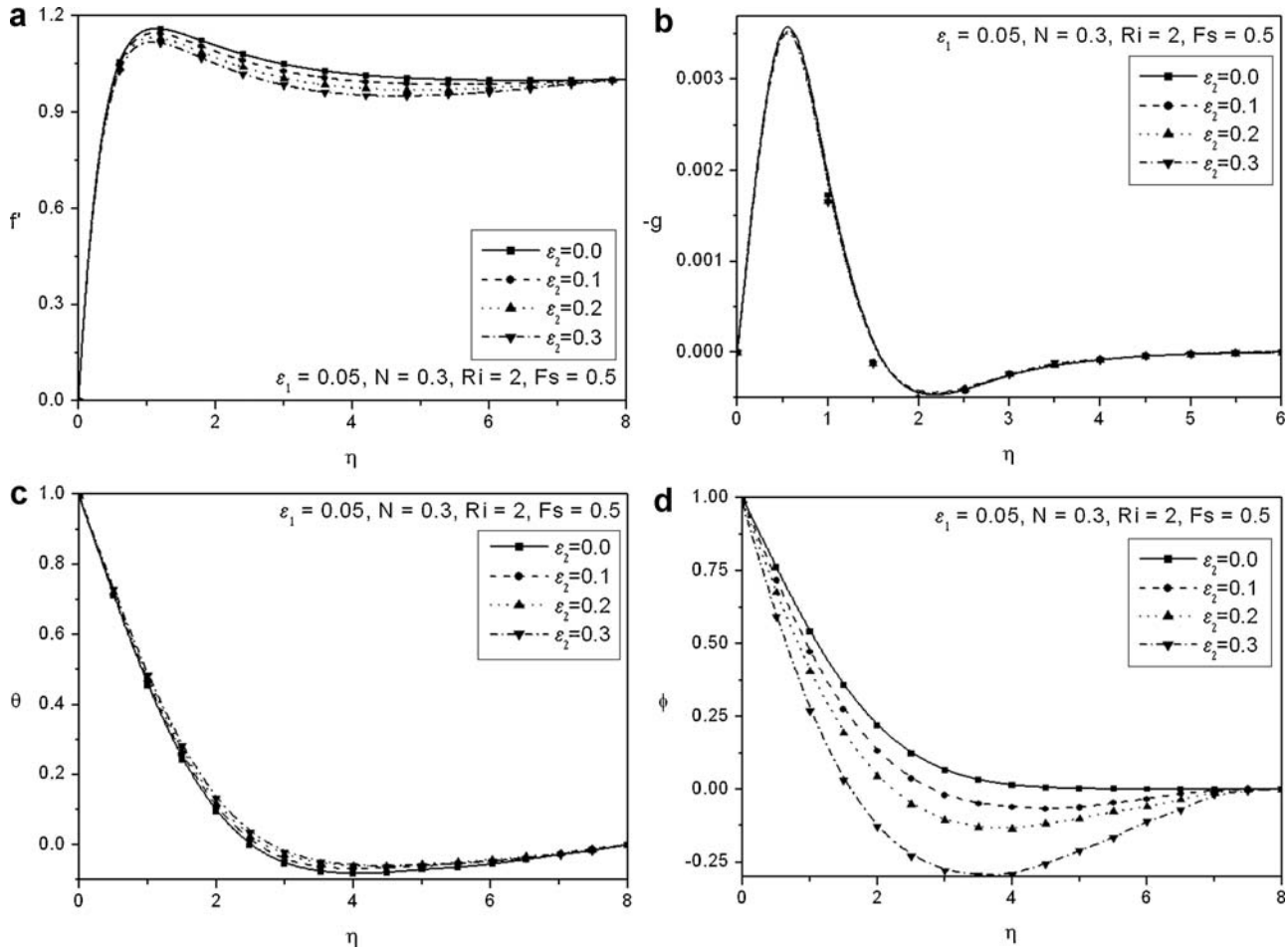

Figure 6. Effect of solutal stratification parameter (ε_2) on the (a) velocity, (b) microrotaion, (c) temperature and (d) concentration.

and mass transfer coefficients against the thermal stratification parameter ε_1 and solutal stratification parameter ε_2 is presented in Table 4. It can be seen that, for fixed values of ε_1 and ε_2, the non-dimensional heat and mass transfer coefficients increase with the increase of *Ri*. Hence, the non-Darcy parameter has an important role in controlling the flow field.

The effect of *Ri* on the non-dimensional heat and mass transfer coefficients with variation of the thermal stratification parameter ε_1 and solutal stratification parameter ε_2 for fixed $N = 0.3$ and $Fs = 0.5$ is presented in Table 5. It can be noticed that the heat transfer coefficient is increasing and the mass transfer coefficient decreases with the increase of ε_1 for fixed values of *Ri* and ε_2. The reverse trend can be seen in the case of ε_2. The effects of buoyancy parameter *Ri* on the non-dimensional heat and mass transfer coefficients against the thermal stratification parameter ε_1 and solutal stratification parameter ε_2 is presented in Table 5. It can be observed that, for fixed values of ε_1 and ε_2, the non-dimensional heat and mass transfer coefficients increase with the increase of *Ri*. Hence the mixed convection parameter has an important role in controlling the temperature and concentration.

Table 3. Variation of non-dimensional heat and mass transfer coefficients versus ε_1 and ε_2 for different values of *N* with $Ri = 1$ and $Fs = 0.5$

		$Nu_x Re_x^{-1/2}$				$Sh_x Re_x^{-1/2}$			
ε_1	ε_2	$N = 0.1$	$N = 0.4$	$N = 0.6$	$N = 0.9$	$N = 0.1$	$N = 0.4$	$N = 0.6$	$N = 0.9$
0.00	0.05	0.4030	0.3831	0.3626	0.2928	0.2518	0.2426	0.2326	0.1961
0.05	0.05	0.4096	0.3893	0.3685	0.2972	0.2518	0.2425	0.2325	0.1961
0.10	0.05	0.4163	0.3956	0.3744	0.3016	0.2518	0.2425	0.2325	0.1961
0.20	0.05	0.4296	0.4082	0.3862	0.3105	0.2517	0.2424	0.2324	0.1960
0.40	0.05	0.4561	0.4333	0.4098	0.3282	0.2515	0.2422	0.2322	0.1959
0.05	0.0	0.4097	0.3894	0.3685	0.2972	0.2493	0.2402	0.2303	0.1947
0.05	0.1	0.4096	0.3893	0.3684	0.2972	0.2543	0.2449	0.2347	0.1976
0.05	0.2	0.4095	0.3892	0.3683	0.2971	0.2593	0.2495	0.2390	0.2004
0.05	0.3	0.4093	0.3891	0.3682	0.2970	0.2642	0.2542	0.2434	0.2033
0.05	0.5	0.4091	0.3889	0.3680	0.2969	0.2742	0.2635	0.2520	0.2091

Table 4. Variation of non-dimensional heat and mass transfer coefficients versus ε_1 and ε_2 for different values of Fs with $N = 0.3$ and $Ri = 2$

ε_1	ε_2	$Nu_x Re_x^{-1/2}$				$Sh_x Re_x^{-1/2}$			
		$Fs = 0.1$	$Fs = 0.5$	$Fs = 1$	$Fs = 2$	$Fs = 0.1$	$Fs = 0.5$	$Fs = 1$	$Fs = 2$
0.00	0.05	0.3557	0.3969	0.4202	0.4428	0.2272	0.2492	0.2616	0.2729
0.05	0.05	0.3612	0.4034	0.4273	0.4504	0.2271	0.2491	0.2615	0.2729
0.10	0.05	0.3666	0.4099	0.4344	0.4581	0.2270	0.2490	0.2615	0.2728
0.20	0.05	0.3775	0.4228	0.4485	0.4734	0.2267	0.2489	0.2614	0.2728
0.30	0.05	0.3991	0.4486	0.4767	0.5040	0.2261	0.2485	0.2611	0.2726
0.05	0.00	0.3613	0.4035	0.4274	0.4505	0.2252	0.2467	0.2588	0.2699
0.05	0.10	0.3610	0.4033	0.4272	0.4504	0.2291	0.2515	0.2642	0.2758
0.05	0.20	0.3606	0.4031	0.4271	0.4503	0.2329	0.2563	0.2696	0.2817
0.05	0.30	0.3602	0.4029	0.4270	0.4502	0.2368	0.2612	0.2749	0.2876
0.05	0.50	0.3594	0.4024	0.4267	0.4501	0.2445	0.2708	0.2857	0.2993

Table 5. Variation of non-dimensional heat and mass transfer coefficients versus ε_1 and ε_2 for different values of Ri with $N = 0.3$ and $Fs = 0.5$

ε_1	ε_2	$Nu_x Re_x^{-1/2}$				$Sh_x Re_x^{-1/2}$			
		$Ri = 0.5$	$Ri = 1$	$Ri = 1.5$	$Ri = 2$	$Ri = 0.5$	$Ri = 1$	$Ri = 1.5$	$Ri = 2$
0.00	0.05	0.3875	0.3907	0.3939	0.3969	0.2446	0.2462	0.2477	0.2492
0.05	0.05	0.3939	0.3971	0.4003	0.4034	0.2446	0.2461	0.2476	0.2491
0.10	0.05	0.4003	0.4036	0.4068	0.4099	0.2446	0.2461	0.2476	0.2490
0.20	0.05	0.4131	0.4164	0.4197	0.4228	0.2445	0.2460	0.2474	0.2489
0.30	0.05	0.4259	0.4293	0.4325	0.4357	0.2445	0.2459	0.2473	0.2487
0.05	0.00	0.3939	0.3972	0.4004	0.4035	0.2422	0.2437	0.2452	0.2467
0.05	0.10	0.3938	0.3971	0.4002	0.4033	0.2470	0.2485	0.2500	0.2515
0.05	0.20	0.3938	0.3970	0.4001	0.4031	0.2518	0.2533	0.2549	0.2563
0.05	0.30	0.3937	0.3969	0.3999	0.4029	0.2565	0.2581	0.2597	0.2612
0.05	0.50	0.3936	0.3966	0.3996	0.4024	0.2661	0.2677	0.2693	0.2708

CONCLUSIONS

In this study, a boundary layer analysis for mixed convection in a doubly stratified micropolar fluid saturated non-Darcy porous medium in the presence of uniform wall temperature and concentration is presented. Using the pseudo-similarity variables, the governing equations are transformed into a set of non-similar parabolic equations where numerical solution has been presented for a wide range of parameters.

- The higher values of the coupling number N (i.e. for the case where the effect of microstructure becomes significant) resulting in lower velocity and microrotation distributions but higher wall temperature, wall concentration distributions in the boundary layer compared to the Newtonian fluid case ($N = 0$). The numerical results indicate that the skin friction and wall couple stresses in micropolar fluids are less than those obtained with Newtonian fluids. Also, non-dimensional heat and mass transfer coefficients decrease with the increase of the coupling number.
- An increase in Fs decrease in velocity and wall couple stress accompanied by an increase in temperature and concentration distributions, heat and mass transfer rates and the local skin friction factor.
- An increase in Ri, enhanced velocity, skin friction parameter and non-dimensional heat and mass transfer coefficients but reduction in microrotation, temperature and concentration distributions and in wall couple stress in boundary layer.
- An increase in thermal stratification parameter ε_1, reduction in velocity, temperature distributions, skin friction parameter and non-dimensional mass transfer coefficient but increase in non-dimensional heat transfer coefficient, concentration distribution and wall couple stress in boundary layer.
- An increase in solutal stratification parameter ε_2, reduction in velocity, concentration distributions, skin friction parameter and non-dimensional heat transfer coefficient but increase in temperature distribution, non-dimensional mass transfer coefficient and wall couple stress in boundary layer.
- We observe that the microrotation changes sign from negative to positive values within the boundary layer in the presence of stratification. The results also indicate that skin friction and wall couple stresses are reduced in the case of micropolar fluid when compared with the case of Newtonian fluid.

NOMENCLATURE

A	slope of ambient temperature
B	slope of ambient concentration
$\mathcal{B}$	buoyancy ratio
b	coefficient in the Forchheimer term
C	concentration (kmol m^{-3})

C_w wall concentration (kmol m^{-3})
C_f skin friction coefficient
$C_{\infty,0}$ ambient concentration (kmol m^{-3})
D solutal diffusivity (m^2 s^{-1})
Da Darcy number
g^* gravitational acceleration (m s^{-2})
g dimensionless microrotation
Gr thermal Grashof number
f reduced stream function
j microinertia density (kg m^{-3})
J dimensionless microinertia density
k thermal conductivity (W m^{-1} K^{-1})
L characteristic length (m)
M_w dimensionless wall couple stress
m_w wall couple stress (Pa m^{-1})
Nu_x local Nusselt number
N coupling number
Pr Prandtl number
Re Reynolds number
Re_x local Reynolds number
Ri mixed convection parameter
Sc Schmidth number
Sh_x local Sherwood number
T temperature (K)
T_w wall temperature (K)
$T_{\infty,0}$ ambient temperature (K)
U_* characteristic velocity
u,v velocity components in x and y directions (m s^{-1})
u_∞ free stream velocity (m s^{-1})
x,y coordinates along and normal to the plate (m)
α thermal diffusivity (m^2 s^{-1})
β_T, β_C coefficients of thermal and solutal expansion (K^{-1}, K^{-1})
γ spin-gradient viscosity (m^2 s^{-1})
η pseudo-similarity variable (m)
θ dimensionless temperature
ϕ dimensionless concentration
κ vortex viscosity (m^2 s^{-1})
λ dimensionless spin-gradient viscosity
μ dynamic viscosity (kg m^{-1} s^{-1})
ν kinematic viscosity (m^2 s^{-1})
ξ dimensionless streamwise coordinate
ρ density of the fluid (kg m^{-3})
τ_w wall shear stress (Pa)
ψ stream function
ω component of microrotation
ε_1, ε_2 thermal and solutal stratification parameters

Subscripts

w wall condition
∞ ambient condition
C concentration
T temperature

Superscript

$'$ differentiation with respect to η

ACKNOWLEDGEMENTS

The authors are thankful to the reviewers for their valuable suggestions and comments.

REFERENCES

Awad, F. and P. Sibanda, ''Dufour and Soret Effects on Heat and Mass Transfer in a Micropolar Fluid in a Horizontal Channel,'' WSEAS Trans. Heat Mass Transf. **5**, 165–177 (2010).

Cebeci, T. and P. Bradshaw, ''Physical and Computational Aspects of Convective Heat Transfer,'' Springer-Verlin, New York (1984).

Chang, C. L. and Z. Y. Lee, ''Free Convection on a Vertical Plate With Uniform and Constant Heat Flux in a Thermally Stratified Micropolar Fluid,'' Mech. Res. Commun. **35**, 421–427 (2008).

Cowin, S. C., ''Polar Fluids,'' Phys. Fluids **11**, 1919–1927 (1968).

Eringen, A. C., ''Theory of Micropolar Fluids,'' J. Math. Mech. **16**, 1–18 (1966).

Gebhart, B., Y. Jaluria, R. Mahajan and B. Sammakia, ''Buoyancy lnduced Flows and Transport,'' Hemisphere Publishing Co., New York (1988).

Gorla, R. S. R., P. P. Lin and A.-J. Yang, ''Asymptotic Boundary Layer Solutions for Mixed Convection From a Vertical Surface in a Micropolar Fluid,'' Int. J. Eng. Sci. **28**, 525–533 (1990).

Gorla, R. S. R., A. J. Chamkha and Md. A. Hossain, ''Mixed Convection Flow of Non-Newtonian Fluid From a Slotted Vertical Surface With Uniform Surface Heat Flux,'' Can. J. Chem. Eng. **87**(4), 534–540 (2009).

Jaluria, Y. and B. Gebhart, ''Stability and Transition of Buoyancy Induced Flows in a Stratified Medium,'' J. Fluid Mech. **66**, 593–612 (1974).

Jaluria, Y. and K. Himasekhar, ''Buoyancy Induced Two Dimensional Vertical Flows in a Thermally Stratified Environment,'' Comput. Fluids **11**, 39–49 (1983).

Jena, S. K. and M. N. Mathur, ''Mixed Convection Flow of a Micropolar Fluid From an Isothermal Vertical Plate,'' Comput. Math. Appl. **10**, 291–304 (1984).

Lakshmi Narayana, P. A. and P. V. S. N. Murthy, ''Free Convective Heat and Mass Transfer in a Doubly Stratified Non-Darcy Porous Medium,'' J. Heat Transf. **128**, 1204–1212 (2006).

Lakshmi Narayana, P. A. and P. V. S. N. Murthy, ''Soret and Dufour Effects on Free Convection Heat and Mass Transfer in a Doubly Stratified Darcy Porous Medium,'' J. Porous Media **10**, 613–623 (2007).

Lloyd, J. R. and E. M. Sparrow, ''Combined Free and Forced Convective Flow on Vertical Surfaces,'' Int. J. Heat Mass Transf. **13**, 434–438 (1970).

Motsa, S. S., S. Shateyi and P. Sibanda, ''A Model of Steady Viscous Flow of a Micropolar Fluid Driven by Injection or Suction Between a Porous Disk and a Non-Porous Disk Using a Novel Numerical Technique,'' Can. J. Chem. Eng. **88**(6), 991–1002 (2010).

Murthy, P. V. S. N., D. Srinivasacharya and P. V. S. S. S. R. Krishna, ''Effect of Double Stratification on Free Convection in Darcian Porous Medium,'' J. Heat Transf. **126**, 297–300 (2004).

Murthy, P. V. S. N., S. Mukherjee, P. V. S. S. S. R. Krishna and D. Srinivasacharya, ''Mixed Convection Heat and Mass Transfer in a Doubly Stratified Non-Darcy Porous Medium,'' Int. J. Appl. Mech. Eng. **12**, 109–123 (2007).

Nield, D. A. and A. Bejan, ''Convection in Porous Media,'' 3rd ed., Springer-Verlag, New York (2006).

Prandtl, L., ''Essentials of Fluid Dynamics,'' Blackie, London (1952).

Rahman, M. M. and M. Al-Lawatia, ''Effects of Higher Order Chemical Reaction on Micropolar Fluid Flow on a Power Law Permeable Stretched Sheet With Variable Concentration in a Porous Medium,'' Can. J. Chem. Eng. **88**(1), 23–32 (2010).
Ranganathan, P. and R. Viskanta, ''Mixed Convection Boundary Layer Flow Along a Vertical Porous Medium,'' Numer. Heat Transf. **7**, 305–317 (1984).
Rathish Kumar, B. V. and Shalini, ''Double Diffusive Natural Convection in a Doubly Stratified Wavy Porous Enclosure,'' Appl. Math. Comput. **171**, 180–202 (2005).
Shateyi, S., S. S. Motsa and P. Sibanda, ''Homotopy Analysis of Heat and Mass Transfer Boundary Layer Flow Through a Non-Porous Channel With Chemical Reaction and Heat Generation,'' Can. J. Chem. Eng. **88**(6), 975–982 (2010).
Srinivasacharya, D. and Ch. RamReddy, ''Heat and Mass Transfer by Natural Convection in a Doubly Stratified Non-Darcy Micropolar Fluid,'' Int. Commun. Heat Mass Transf. **37**, 873–880 (2010).
Srinivasacharya, D. and Ch. RamReddy, ''Soret and Dufour Effects on Mixed Convection in a Non-Darcy Porous Medium Saturated With Micropolar Fluid,'' Nonlinear Anal. Model. Control **16**, 100–115 (2011).
Vafai, K. and C. L. Tien, ''Effect of Mass Transfer on Free Convective Flow of a Dissipative Incompressible Fluid Past an Infinite Vertical Porous Plate With Suction,'' Proc. Ind. Acad. Sci. **84A**, 194–203 (1976).
Wang, T.-Y., ''The Coupling of Conduction With Mixed Convection of Micropolar Fluids Past a Vertical Flat Plate,'' Int. Commun. Heat Mass Transf. **25**, 1075–1084 (1998).

Manuscript received February 20, 2011; revised manuscript received April 15, 2011; accepted for publication May 10, 2011.